5th International Conference on Experimental Fluid Mechanics ICEFM 2018 Munich
Munich, Germany, July 2-4, 2018

Design of a high-speed focusing schlieren system for complex three-dimensional flows

Christopher Schauerte[1], **Anne-Marie Schreyer**[1*]

[1] RWTH Aachen University, Institute of Aerodynamics, 52062 Aachen, Germany

[*] a.schreyer@aia.rwth-aachen.de

Abstract

A large-field focusing schlieren system was designed for non-intrusive measurements in complex high-speed flows. Different image acquisition techniques were investigated, evaluating the system performance with respect to depth of focus, sensitivity, and field of view. The influence of these parameters was shown based on the analysis of a separated 24° compression ramp interaction at Mach 2.5, also demonstrating the advantages of the focusing schlieren technique when analyzing three-dimensional flow fields. Variations of the flow topology in the spanwise direction become distinguishable by focusing on different spanwise planes. In order to optically resolve dynamic flow phenomena, time-resolved series of images were recorded with a high-speed camera at a frame rate of 20 kHz. The suitability of the recorded image sequences for post-processing with dynamic mode decomposition to extract the dynamically relevant structures as well as their characteristic frequencies is demonstrated and discussed.

1 Introduction

One of the major issues in aerospace transportation, especially in the context of transonic and supersonic flight, is a stable and predictable flow configuration. Shock wave boundary layer interactions (SWBLI) are phenomena which inescapably occur in these flight regimes. Turbulent boundary layers interacting with oblique shock waves are susceptible to flow separation, creating a highly unsteady three-dimensional flow field, potentially leading to buffeting or severe local thermal loads (Délery and Marvin (1986)). Since these interactions occur in various applications such as transonic airfoils and inlets of air-breathing engines, they are a research topic of high interest. To be able to effectively control and alleviate the detrimental effects of shock induced separation, we require a better understanding of the mechanisms that govern such interactions. Coherent turbulent structures and low-frequency phenomena characterize these flows (see for example Dupont et al. (2006); Clemens and Narayanaswamy (2014) and Délery and Marvin (1986)). To optically resolve such events, we required an experimental setup producing sharp time-resolved visualization sequences of two-dimensional planes across the entire flow field. Based on these images, we intend to a) analyze the instantaneous and averaged flow topology, and b) analyze the governing flow dynamics by applying Dynamic Mode Decomposition (DMD) (Schmid et al. (2011)). Schlieren techniques, which are based on the visualization of density gradients in transparent media, have the advantage of not interfering with the considered flow field (Settles (2001)). Previously, conventional schlieren arrangements were applied for the visualization of large-field wind tunnel flows. While these systems are relatively easy to set up, they typically require large-scale optics of extraordinarily high quality (Burton (1949)). An aspect of even greater importance is that these system are characterized by an enormous depth of field, resulting in an integrated image of all schlieren phenomena occuring along the optical path (Kantrowitz and Trimpi (1950)). This precludes the detailed examination of highly three-dimensional flows such as SWBLI (Fish and Parnham (1951)). To overcome this, we designed a focusing schlieren system, that gives optical access to selected spanwise planes across the flow field and thus allows to identifiy spanwise variations in the flow topology (Weinstein (1993)). To assess the true benefits of the newly designed system, the characteristics are compared to a classical schlieren approach in terms of sensitivity, depth of focus (DOF) and the obtainable field of view (FOV), and a 24° compression ramp interaction at Mach 2.5 is analyzed.

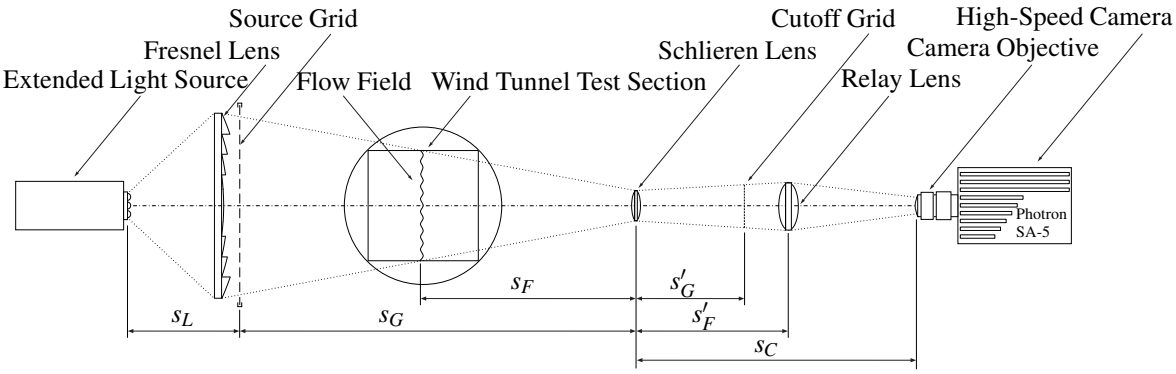

Figure 1: Schematic of the focusing schlieren arrangement with optical relay system (s_L=623 mm, s_G=3189 mm, s'_G=591 mm, s_F=1510 mm, s'_F=787 mm, and s_C=1032 mm

2 Experimental setup and conditions

2.1 Wind tunnel facility and model

All experiments were performed in the trisonic wind tunnel at the Institute of Aerodynamics, RWTH Aachen University, at a Mach number of 2.5 and a Reynolds number of $9.96 \cdot 10^6$ 1/m. The intermittent wind tunnel allows to perform measurements at subsonic, transonic and supersonic flow conditions. Supersonic Mach numbers are set with the variable Laval nozzle. Using vacuum tanks with a total capacity of 4 x 95 m^3, the indraft facility is operated with dried air from a reservoir with a volume of 165 m^3. The ambient conditions determine the stagnation pressure and temperature, the selected Mach number thus sets the Reynolds number. With the present setup and conditions a stationary measurement period of approximately 3.5 seconds is obtained. The facility has a rectangular test section of 400 x 400 mm^2. Optical access is provided by circular windows with a diameter of 280 mm on both side walls. A fully-separated SWTBLI is generated by installing a 24° compression ramp on a flat plate model installed on the test-section center line.

2.2 Focusing schlieren optical system

Schlieren arrangements based on extended grids illuminated by correspondingly large illuminated surfaces instead of point-shaped light sources were discussed in great detail with regard to the intrinsic advantages by Schardin (1942) as early as in the 1940s. These systems were originally devised to cover a field of view larger than the aperture of the employed optics. Fish and Parnham (1951) were the first to provide a mathematical study of the properties and limitations of such systems. Similar arrangements based on multiple light sources were devised by Burton (1949) as well as Kantrowitz and Trimpi (1950). Boedeker (1959) first proposed the use of a Fresnel lens, leading to a dramatically increased light intensity. Weinstein (1993) devised an approach to generate a modern-type version with the characteristic ability to bring specific planes along the optical axis into focus (Settles (2001)). This feature allows the differentiation and investigation of narrow slices within the flow field and simultaneously prevents disturbances, such as striation in lenses, from influencing the image (Alvi et al. (1993)).

The layout of our focusing schlieren system is shown in Figure 1. A back-lit source grid is mapped onto a corresponding plane coinciding with the cutoff grid position. This secondary grid resembles an accurate negative image of the source grid, whereby an infinitely variable adjustment of the amount of cutoff is obtained (Fish and Parnham (1951)). In this manner many individual pairs of source slits and corresponding opaque stripes in the cutoff region work as independent schlieren systems (VanDercreek et al. (2010)). Consequently, the test section is intersected by a large number of light cones, each of them working at a different inclination with reference to the optical axis. Irregular light rays, distracted from their original path by density gradients, either pass the individual "knife-edges" or are blocked, dependent on the amount and orientation of deflection. These rays appear as brighter or darker points on the screen. Due to the multiple-source approach, objects in the flow field are reproduced by a number of superposed images. For a fixed position of the screen, the points of one specific object plane coincide exactly, forming an utterly sharp image (Kantrowitz and Trimpi (1950)). Objects outside of the focal plane appear blurred, which results in the characteristic limited depth of field. Weinstein (1993) quantified the focusing effect, introducing the

depth of sharp focus DS and the depth of unsharp focus DU. The latter term (see eq. (1)) takes into account that the focusing effect is primarily determined by the ratio l/A, with the distance l between the object under investigation and the main focusing lens and the clear aperture A of this lens. (Fish and Parnham (1951)).

$$DU \propto \frac{s_F}{A} \tag{1}$$

The system performance is defined by the detectability limit of changes in the refractive index. Weinstein (1993) defined the sensitivity

$$\varepsilon_{min} = 20626 \frac{a s_G}{s'_G (s_G - s_F)} \text{arcsec}, \tag{2}$$

which corresponds to the smallest detectable angular deflection of light rays, based on the assumption that the lowest perceptible change of brightness is 10%. a is the height of the light slit above the cutoff. For the remaining quantities see Fig. 2.

The setup of the current focusing schlieren setup was influenced by numerous factors and requirements related to the flow field and desired field of view, as well as geometric constraints in the experimental facility. Another major aspect was the availability of adequate optical components, which determine the system performance in terms of resolution, sensitivity and depth of focus.

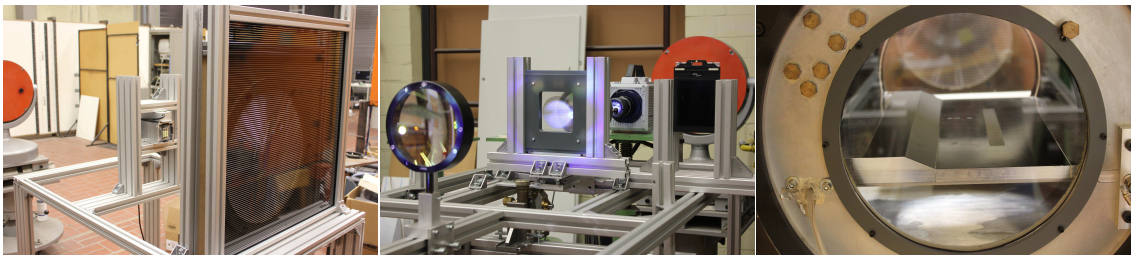

Figure 2: Left and middle: Focusing schlieren setup, including the extended light source, Fresnel lens, source grid, main focusing lens, cutoff grid and the optical setup projecting the image into the camera. Right: Flat-plate and compression ramp model installed in the wind tunnel test section.

An evenly illuminated, large-scale field of view covering the entire compression ramp interaction and parts of the upstream boundary layer was realized with large-scale light source grids, consisting of alternating clear and opaque stripes (see Figure 2 (left)). The quadratic source grids with a side length of 690 mm are custom made of light-tight black adhesive foil attached to 4 mm thin sheets of white glass, reducing the loss of light to a minimum. The large mirrors used in conventional schlieren (Settles (2001)) are substituted with a single plano-convex schlieren lens with a focal length of 500 mm and a clear aperture of 150 mm. This lens projects a rescaled image of the source grid onto the image plane, where the illuminated stripes are partially blocked by a corresponding cutoff grid. This cut-off grid needs to be an exact photographic negative of the source grid (see Weinstein (1993)). To obtain the best possible accuracy, the grid was generated by exposing photosensitive sheet films (4x5 inch medium sensitive b/w films (Ilford Delta 100)) with the sharply focused image of the source grid. An extended light source consisting of a 3x3 array of Cree XLamp 15 W cool-white high-power LEDs was designed such that its sharp image covers the entire clear aperture of the main lens when refocused by the 470 mm Fresnel lens. A Meanwell HLG-120H constant current source with a maximum output of 10 A and 120 W was used for constant and intense illumination of the field of view. A Photon Fastcam SA5 CMOS camera was used to record images with a spatial resolution of 704×520 pixels at a frame rate of 20 kHz. This is sufficient to capture the low-frequency oscillation of the shock and separation bubble system as well as the large-scale turbulent structures in the boundary layer (see Dupont et al. (2006)).

3 Validation of the system

3.1 System characteristics

The image sensitivity in our current setup reaches a value of $\varepsilon_{min} = 6.14$ arcsec. The general system performance depends partially on the image-capturing technique. The largest possible field of view with a

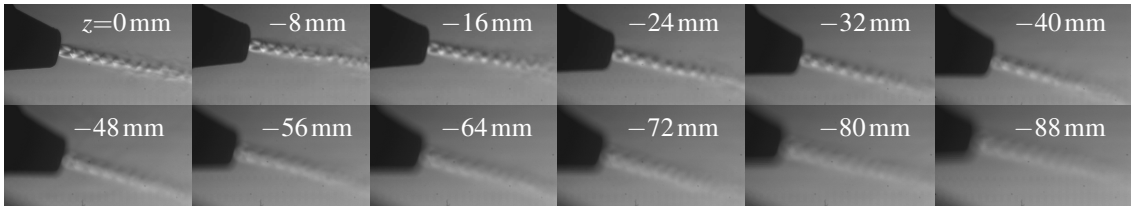

Figure 3: Focusing schlieren images of a jet of compressed air directly focused on the camera sensor at different spanwise locations ($z = 0$ corresponds to the jet center line).

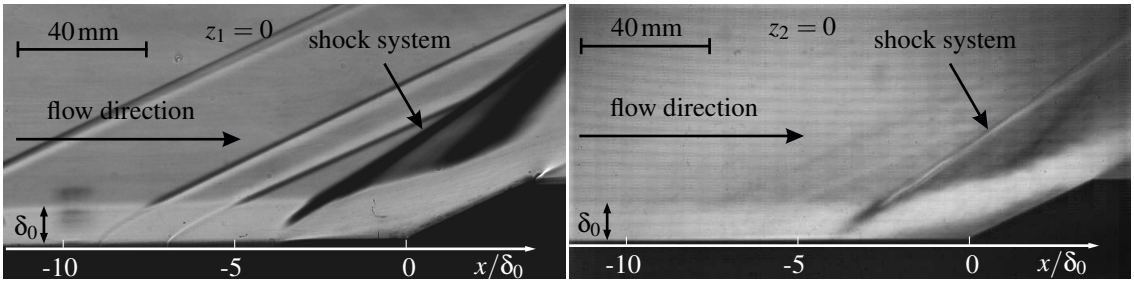

Figure 4: Classical (left) and focusing schlieren images focused on the model center line (right) of a 24° compression-ramp interaction at Mach 2.5.

diameter of 280 mm can be reached when directing the entire cone of light into the camera with a system of lenses (see Figure 1). This is congruent with the FOV of a conventional schlieren setup. A major disadvantage of such a relay lens is an increase in depth of focus. To achieve the minimal depth of focus, the image can be focused directly onto the camera sensor. This leads, however, to a significant reduction of the field of view, since only a small image region is covered by the sensor. To visualize the defocusing ability of the system, the expanding jet of an airgun is depicted in Figure 3. For a fixed focal position, the airgun was incrementally moved in the spanwise direction. Significant blurring of flow features begins with an axial shift of 8 mm, defined structures are no longer detectable for an offset of 40 mm. This agrees with the calculated focusing performance and DU of the present system.

3.2 Application in a separated compression-ramp interaction

To assess the quality of the developed system in the desired field of application, complex compressible flows, measurements were carried out in a separated 24° compression-ramp interaction at Mach 2.5. A classical schlieren image and a focusing schlieren image taken with the setup including the relay lens (larger FOV) are shown in Figure 4 (left) and (right), respectively. In both cases, the incoming boundary layer and the typical structure of separation and reattachment shocks can be observed. The lambda shock structure is more distinct and less smeared out in the focusing schlieren image. Flow disturbances and weak Mach waves induced by small local discontinuities in the model surface (pressure taps, for example) outside of the focusing plane, however, are much less prominent in the focusing schlieren image, while the classical schlieren image contains all disturbances occurring along the entire light path. The more relevant features of the flow topology are thus easier to recognize in the focusing schlieren image. Note that the classical schlieren image was taken with a Canon EOS 550D reflex camera and is therefore more crisp than the focusing schlieren images taken with the Photon Fastcam SA5.

The relevance of a limited depth of field becomes even more obvious when considering the strongly three-dimensional flow field of a SWBLI with separation control. In order to decrease shock-induced flow separation, small air jets were injected into the boundary layer from circular orifices in the model surface upstream of the interaction, which introduced longitudinal vortices. As a result, the separation line is not only shifted, but strongly corrugated, as can be observed from the cutouts of oil surface-flow visualizations in Figure 5 (left), showing the separation line. The local shock position thus varies in the spanwise direction. While all local shock locations are depicted equally strong in a classical schlieren image due to the nature of the technique (not shown), the minimum and maximum shock location is visible in the two focusing schlieren images shown in Figure 5 (center and right). These images were projected onto the camera sen-

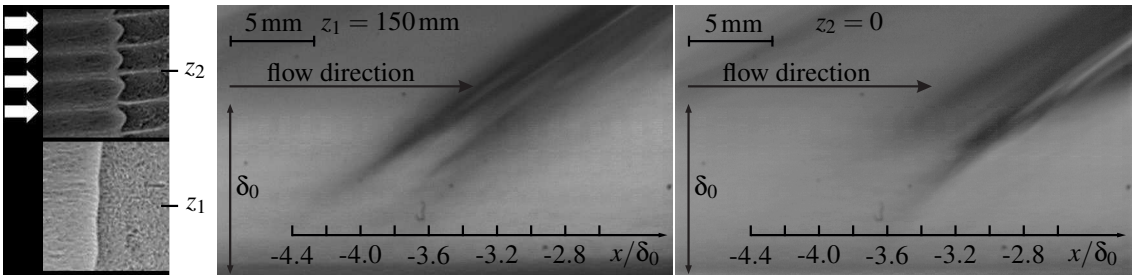

Figure 5: Left: Oil-flow visualization cutouts of the separation line upstream of the ramp corner. White arrows mark the location of jet orifices. Center and right: Focusing schlieren images of the separation shock at spanwise locations downstream of a jet orifice (right) and far away from the control inlet (center).

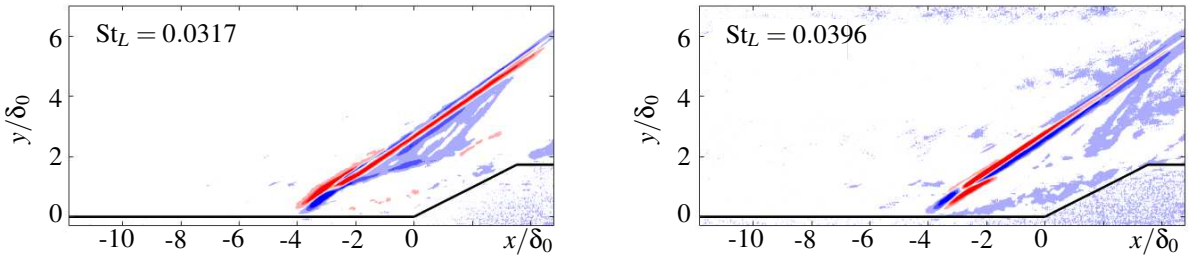

Figure 6: Exemplary dynamic modes (real part only) representative for the motion of the separation shock.

sor directly to profit from the narrower depth of focus. For the image in Figure 5 (center), the system was focused on a plane far away from the model center line, where no air jets were introduced. Consequently, the separation shock at its furthest upstream location ($x/\delta_0 = -4.4$) is most distinct. In the image in Figure 5 (right) on the other hand, which was focused on the jet orifice on the model center line, this shock is only a rather weak shadow, while the shock at the local focusing plane is nicely visible ($x/\delta_0 = -3.6$).

3.3 Post-processing with DMD

To assess the suitability of our data for further analysis of the flow dynamics, we applied a dynamic mode decomposition (DMD), as introduced by Schmid et al. (2011) and Jovanović et al. (2014), to a recorded image sequence of the uncontrolled compression ramp interaction. DMD allows for a modal analysis of a data sequence without requiring an underlying model and is therefore applicable to experimental data. The resulting modes represent the dominant dynamic behavior of the flow field captured in the snapshots, providing both their spacial shape and characteristic frequency. Schlieren images give access to one flow quantity only and do therefore not allow an investigation of the complete dynamic behavior of the flow as numerical data sets would. The strong density gradients across the shock wave, however, can be nicely captured with schlieren visualizations. This gives access to the dynamics of the shock system and thus the phenomenon of the low-frequency shock unsteadiness, which is one of the central phenomena of interest related to shock wave / boundary layer interactions with separation.

We apply DMD to a sequence of 300 schlieren snapshots recorded at the model centerline, equispaced in time with a delay of $dt = 50\,\mu$s, and thus allowing to resolve Strouhal numbers between $0.012 \leq St_L \leq 0.46$. The sampling interval was chosen such that the low-frequency unsteadiness, which occurs typically around $St_L = 0.03$ (Dupont et al. (2006)), could be captured. $St_L = \frac{f \cdot L}{U_\infty}$ was calculated based on the separation length L, which was determined from surface oil-flow visualizations. Two dominant DMD modes for $St_L = 0.0317$ and $St_L = 0.0396$ are shown in Figure 6. The modes do indeed represent the up- and downstream motion of the shock system. Several modes in the range around $St_L = 0.03$ contribute to this motion, which is a typical observation for this phenomenon (see Nichols et al. (2016).) The quality of the focusing schlieren images yields very distinct spatial mode representations at the respective spanwise location. Analyzing three-dimensional flow fields, and possible spanwise variations therein, is therefore feasible.

4 Conclusion

A focusing schlieren system to visualize complex high-speed flows was designed and applied to a separated compression-ramp interaction at Mach 2.5. The system resolves spanwise variations in such flow fields, which are inaccessible for classical schlieren methods. We recorded image sequences for various spanwise locations with a high-speed camera. The suitability of the image sequences for post-processing with dynamic mode decomposition was demonstrated and the low-frequency unsteadiness of the shock system could be clearly extracted. This shows the potential of the measurement technique for the analysis of the dynamics of such three-dimensional flows at much lower cost and experimental effort than with other techniques.

Acknowledgements

This work was funded by the German Research Foundation (DFG) in the framework of the Emmy Noether Programme (grant SCHR 1566/1-1). The authors wish to thank Ivo Mayr (Department of Visual Arts) for his support related to the film development process and Volker Hansen for the programming of the flash exposure panel. The contributions of Nick Capellmann and the workshop are gratefully acknowledged.

References

Alvi FS, Settles GS, and Weinstein LM (1993) A sharp-focusing schlieren optical deflectometer. *31st Aerospace Sciences Meeting*

Boedeker LR (1959) *Analysis and construction of a sharp focussing schlieren system*. Master's thesis. Massachusetts Institute of Technology

Burton RA (1949) A modified schlieren apparatus for large areas of field. *J Opt Soc Am* 39:907–908

Clemens NT and Narayanaswamy V (2014) Low-frequency unsteadiness of shock wave/turbulent boundary layer interactions. *Annual Review of Fluid Mechanics* pages 469–492

Délery JM and Marvin JG (1986) Shock-wave boundary layer interactions, agardograph no.280. Technical report. NATO Advisory Group for Aerospace Research and Development

Dupont P, Haddad C, and Debiève JF (2006) Space and time organization in a shock-induced separated boundary layer. *Journal of Fluid Mechanics* pages 255–277

Fish R and Parnham K (1951) Focusing schlieren systems, ministry of supply, aeronautical research council. *Aeronautical Research Council Current Papers*

Jovanović MR, Schmid PJ, and Nichols JW (2014) Sparsity-promoting dynamic mode decomposition. *Physics of Fluids* 26

Kantrowitz A and Trimpi RL (1950) A sharp-focusing schlieren system. *Journal of the Aeronautical Sciences* 17:311–314

Nichols JW, Larsson J, Bernardini M, and Pirozzoli S (2016) Stability and modal analysis of shock/boundary layer interactions. *Theoretical and Computational Fluid Dynamics* pages 1–18

Schardin H (1942) *Schlieren Methods and their Applications*. volume 20 of *Ergebnisse der exakten Naturwissenschaften*

Schmid PJ, Li L, Juniper MP, and Pust O (2011) Applications of the dynamic mode decomposition. *Theoretical and Computational Fluid Dynamics* 25:249–259

Settles GS (2001) *Schlieren and shadowgraph techniques: visualizing phenomena in transparent media*. Springer

VanDercreek CP, Smith MS, and Yu KH (2010) Focused schlieren and deflectometry at aedc hypervelocity wind tunnel no. 9. *AIAA Paper* 4209:2010

Weinstein LM (1993) Large-field high-brightness focusing schlieren system. *AIAA Journal* 31:1250–1255